arXiv:1804.02170v1 [cond-mat.soft] 6 Apr 2018

A microscopic field theoretical approach for binary mixtures of active and passive particles

Francesco Alaimo[1, 2] and Axel Voigt[1, 2, 3, a)]

[1)] *Institute of Scientific Computing, Technische Universität Dresden, 01062 Dresden, Germany*

[2)] *Dresden Center for Computational Materials Science (DCMS), 01062 Dresden, Germany*

[3)] *Center of Systems Biology Dresden (CSBD), Pfotenhauerstr. 108, 01307 Dresden, Germany*

We consider a phase field crystal modeling approach for binary mixtures of interacting active and passive particles. The approach allows to describe generic properties for such systems within a continuum model. We validate the approach by reproducing experimental results, as well as results obtained with agent-based simulations, for the whole spectrum from highly dilute suspensions of passive particles to interacting active particles in a dense background of passive particles.

[a)] Corresponding author: axel.voigt@tu-dresden.de.

I. INTRODUCTION

Active systems have been in the focus of intense research for the last decade because they provide deep insights into the self-organization of systems that are intrinsically in a non-equilibrium state such as living matter. Even more interesting are mixtures of active and passive particles. Situations of active particles in crowed environments or passive particles in an active bath resemble the situation in living matter more realistically and might even shed light on the active dynamic processes within a cell[1]. Observed phenomena in mixtures of active and passive particles are e.g. activity-induced phase-separation[2], the formation of large defect-free crystalline domains[3], propagating interfaces[4] but also a transition from diffusive to subdiffusive dynamics[5,6] and suppressed collective motion[7]. To understand this wide span of phenomena is crucial to almost all applications of active systems.

Different ways exist to describe phenomena in active systems theoretically. Typical approaches for active systems consider either the microscopic scale, taking the interactions between the particles into account, or the macroscopic scale, focusing on the emerging phenomena. For reviews on both theoretical descriptions see e.g.[8,9]. Examples for extensions towards mixtures of active and passive particles are summarized in[10] and range from active particles in confined domains[11–13], through active particles moving between fixed or moving obstacles[5,14–17], to binary mixtures of interacting active and passive particles[2–4,18]. All these studies are examples for models on the microscopic scale. In[19,20] a continuum modeling approach was introduced for active systems which combines aspects from the microscopic and the macroscopic scales. The goal of the paper is to extend this approach to mixtures of active and passive particles which will allow to describe generic properties of such systems. We use the model to study the effect of a few active particles in passive systems (active doping)[3,21,22] and how passive particles perturb collective migration in an active bath[5,23–25]. For the first case we observe enhanced crystallization in the passive system, in quantitative agreement with the results of[3]. For the active bath case we investigate how collective migration is affected by a disordered environment. For the special case of immobile passive particles these results are in agreement with[6,7]. However, for mobile passive particles new phenomena and patterns emerge, which ask for experimental validation. Also the intermediate regime of similar fractions of active and passive particles is rich in complex phenomena but much harder to quantify.

II. THE MODEL

The starting point for the derivation of the model is the microscopic field theoretical model for active particles introduced in[20]. It has been validated against known results obtained with minimal agent-based models and proven to be applicable for large scale computations. The model reads in scaled units

$$\begin{aligned} \partial_t \psi &= M_0 \Delta \tfrac{\delta \mathcal{F}_{\mathrm{vpfc}}}{\delta \psi} - v_0 \nabla \cdot (\psi \mathbf{P}) \\ \partial_t \mathbf{P} &= \Delta \left(\alpha_2 \mathbf{P} + C_2 \mathbf{P}^3\right) - \left(\alpha_4 \mathbf{P} + C_4 \mathbf{P}^3\right) - v_0 \nabla \psi - \beta \mathbf{P} \mathbb{1}_{\psi_A \leq 0} \end{aligned} \tag{1}$$

for a one-particle density field $\psi(\boldsymbol{r}, t)$, which is defined with respect to a reference density $\bar{\psi}$, and the polar order parameter $\mathbf{P}(\boldsymbol{r}, t)$, which is related to a coarse-grained velocity field with a typical magnitude v_0 of the self-propulsion velocity. $\mathbf{P}$ is a local quantity that is different from zero only within the peaks of the density field ψ, which is ensured by $\beta > 0$ typically larger than the other terms entering the $\mathbf{P}$ equation. M_0 is the mobility, α_2 and α_4 are two parameters related to relaxation and orientation of the polarization field and C_2 and C_4 are parameters which govern the local orientational ordering. For simplicity we will restrict ourselves to the case $C_2 = C_4 = 0$, which only allows gradients in the density field ψ to induce local polar order. The energy functional $\mathcal{F}_{\mathrm{vpfc}} = \mathcal{F}_{\mathrm{pfc}} + \mathcal{F}_{\mathrm{v}}$ consists of a Swift-Hohenberg energy[26]

$$\mathcal{F}_{\mathrm{pfc}} = \int \left[\frac{1}{4}\psi^4 + \frac{1}{2}\psi(q + (1+\Delta)^2)\psi \right] d\mathbf{r}, \tag{2}$$

with a parameter q related to temperature and a penalization term

$$\mathcal{F}_{\mathrm{v}} = \int H(|\psi|^3 - \psi^3) d\mathbf{r}, \tag{3}$$

with $H \simeq 1500$ to constrain the one-particle density field ψ to positive values. The penalization term $\mathcal{F}_{\mathrm{v}}$ is the essential modification which allows to model individual particles[27–30]. Without this additional term the model can be related to models for active crystals[19,31]. If, in addition, we neglect the coupling with the polar order parameter $\mathbf{P}$ we obtain the classical phase field crystal (PFC) model introduced in[32,33] to model elasticity in crystalline materials. For a detailed derivation of (2) and its relation to classical density functional theory we refer to[34,35]. If the coupling with $\mathbf{P}$ is neglected but the penalization term (3) considered, the model is known as the vacancy PFC (VPFC) model[27].

Various ways have been introduced to extend the classical PFC model towards a second species, thus modeling binary mixtures[29,34]. We adopt one of these approaches for the VPFC model by considering energies for species A and B with

$$\mathcal{F}(\psi_A, \psi_B) = \mathcal{F}^A_{\text{vpfc}}(\psi_A) + \mathcal{F}^B_{\text{vpfc}}(\psi_B) + \mathcal{F}^{AB}_{\text{int}}(\psi_A, \psi_B) \tag{4}$$

where $\mathcal{F}^i_{\text{vpfc}}, i = A, B$ as before and

$$\mathcal{F}^{AB}_{\text{int}}(\psi_A, \psi_B) = \frac{a}{2}\psi_A^2\psi_B^2 \tag{5}$$

an interaction energy with $a > 0$.

In principle both species appearing in (4) could be made active. Our aim is however to simulate binary mixtures of interacting active and passive particles. With this in mind we couple only species A to the polar order parameter $\mathbf{P}$. We further assume $\mathcal{F}^A_{\text{vpfc}} = \mathcal{F}^B_{\text{vpfc}} = \mathcal{F}_{\text{vpfc}}$ and thus e.g. equal size of the active and passive particles. The resulting dynamical equations are

$$\begin{aligned}
\tfrac{\partial \psi_A}{\partial t} &= M_0^A \Delta \left(\tfrac{\delta \mathcal{F}(\psi_A)}{\delta \psi_A} + a\psi_A\psi_B^2 \right) - v_0 \nabla \cdot (\psi_A \mathbf{P}) \\
\partial_t \mathbf{P} &= \alpha_2 \Delta \mathbf{P} - \alpha_4 \mathbf{P} - v_0 \nabla \psi_A - \beta \mathbf{P} \mathbb{1}_{\psi_A \leq 0} \\
\tfrac{\partial \psi_B}{\partial t} &= M_0^B \Delta \left(\tfrac{\delta \mathcal{F}(\psi_B)}{\delta \psi_B} + a\psi_A^2\psi_B \right)
\end{aligned} \tag{6}$$

which define a microscopic field theoretical approach for binary mixtures of interacting active and passive particles. An extension to more than two species, species with different size and interaction potential and active species with different self-propulsion velocities is obvious.

III. RESULTS

We solve equations (6) in two dimensions using a parallel finite element approach[36]. We adopt a block-Jacobi preconditioner[37] that allows us to use a direct solver locally. This is implemented in AMDiS[38,39]. The computational domain is a square of size $L = 200$ with periodic boundary conditions. The initial condition for ψ_A and ψ_B is calculated using a one-mode approximation with lattice distance $d = 4\pi/\sqrt{3}$ for each particle[30], with the centers placed randomly according to a packing algorithm[40]. The $\mathbf{P}$ field is set to zero initially.

Each maxima in the one-particle density fields ψ_A and ψ_B is interpreted as an active or passive particle, respectively. The diameter of the particle is defined by the lattice distance d. We track the particle positions $\mathbf{x}^i_{A,B}(t)$ and use this information to compute the particle

velocities $\mathbf{v}^i_{A,B}(t)$ as the discrete time derivative of two successive maxima. We define the total particle density $\phi = N\sigma/L^2$, with N the total number of particles $N = N_A + N_B$ and $N_{A,B}$ the number of A and B particles, respectively. The parameter $\sigma = \pi(d/2)^2$ is the area occupied by a single particle. The relative density $\phi_A = N_A/N$ corresponds to the fraction of active particles present in the system. For low relative densities ($\phi_A < 0.2$) we are in the regime of active doping, and analyse how a passive system is influenced by the presence of a few active particles. For high relative densities ($\phi_A > 0.7$) we are in the regime of an active bath and study how a few passive particles affect an active system.

We fix the following parameters $(a, v_0, \alpha_2, \alpha_4, \beta, H, q) = (200, 1.5, 0.2, 0.1, 2, 1500, -0.9)$, unless otherwise specified in the figure captions.

A. Active doping: how active particles enhance crystallization

It has been shown by particle simulations[21,22] and experimentally[3] that the crystalline structure of passive particles is altered by the presence of active agents. More precisely active particles generate density variation in the passive system and promote crystallization, leading to the formation of passive clusters. To analyze these phenomena with our microscopic field theoretical approach we need to identify if a particle belongs to a cluster. We follow the definition of[3] where two criteria have to be fulfilled. The nearest neighbor distances less than $3/2d$ and the coordination number is 6.

Figure 1 shows snapshots with passive clusters for different relative and absolute densities, ϕ_A and ϕ, respectively. The time evolution of the percentage of passive particles which belong to a cluster X_f is shown in figure 2. For dilute systems ($\phi = 0.5$, figure 1(a)) X_f slowly increases with time. Increasing the relative density ϕ_A leads to larger values X_f. However, it remains relatively low, rarely exceeding 20%, for the considered time ($t = 1000$). Increasing the density ($\phi = 0.6$, figure 1(b)) the system changes from a state where no clusters are present ($t = 0$) to a state where up to 50% of the passive particles are found in clusters. A maximum X_f is observed for $\phi_A = 0.1$, where X_f saturates at $t = 1000$. Further increasing the number of active particles leads to a reduction of X_f. Adding more and more active particles to systems with already existing crystalline clusters introduces disorder. A phenomena already observed in[3]. By further increasing the density ($\phi = 0.7$, figure 1(c)) some clusters are already present for the random initial configuration at $t = 0$, due to

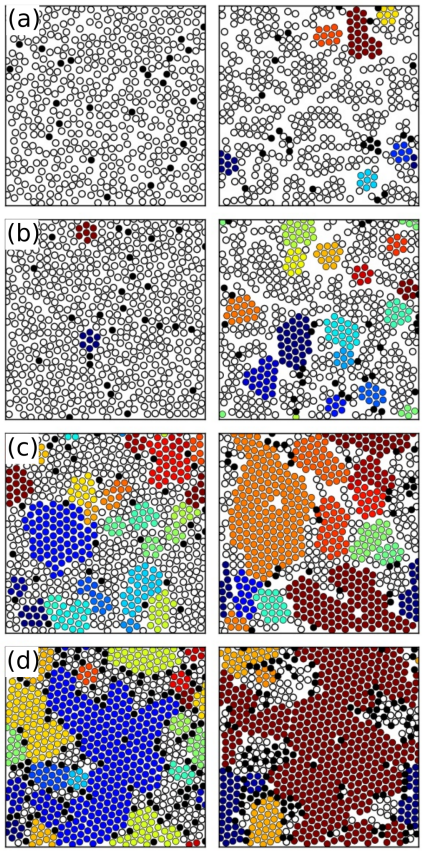

FIG. 1. Snapshots showing passive clusters for different relative and absolute densities at time $t = 0$ (first column) and at time $t = 1000$ (second column). Particles with the same color belong to the same cluster, white disks represents passive particles not belonging to any cluster and black disks are active particles. (a) $\phi = 0.5, \phi_A = 0.05$, (b) $\phi = 0.6, \phi_A = 0.05$ (c) $\phi = 0.7, \phi_A = 0.05$, (d) $\phi = 0.8, \phi_A = 0.15$. Other parameters are $M_0^A = M_0^B = 50$.

spontaneously crystallization. Active particles can be inside these regions, thus disturbing their symmetry. This explains why the system behaves in the opposite way as for the dilute case, with X_f decreasing as the fraction of active particles ϕ_A increases. Finally for $\phi = 0.8$ the initial configuration is already almost completely crystallized ($X_f \simeq 1$ for $t = 0$, figure 1(d)). Adding active particles partially destroys the crystalline structure (figure 2) and X_f decreases for increasing ϕ_A. We thus observe both phenomena, enhanced crystallization in dilute systems and suppressed crystallization in dense systems.

A final observation concerns how the dynamics of the active particles is affected by the presence of passive ones. In figure 3 the maximum displacement d_A for active particles (averaged over all the particles) is shown as a function of the absolute and relative densities

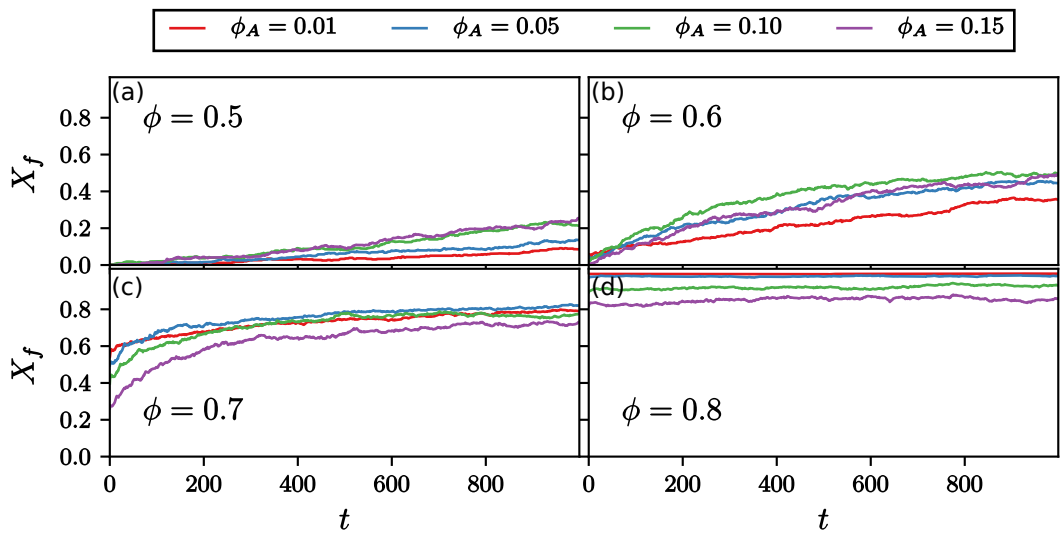

FIG. 2. Percentage of passive particles belonging to a cluster X_f as a function of time for different relative and absolute densities ϕ_A and ϕ. We observe that for $\phi = 0.5$ and $\phi = 0.6$ (top row), increasing the number of active particles lead to an increase of X_f, whereas the opposite is true for $\phi = 0.7$ and $\phi = 0.8$ (bottom row). Other parameters are $M_0^A = M_0^B = 50$. Each curve has been obtained as the average of five different simulations started with different initial conditions.

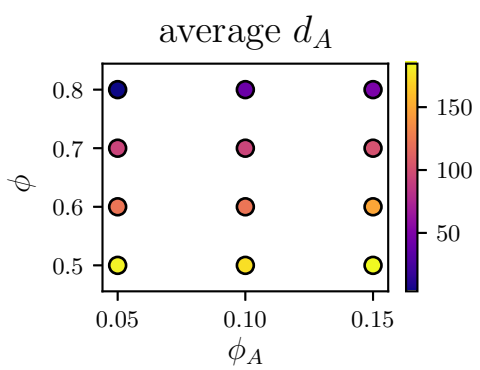

FIG. 3. Average of the maximum displacement d_A of active particles moving in a binary mixture for different values of ϕ and ϕ_A. Active particles travel a longer distance when the passive particles have not crystallized, until the extreme case of $\phi = 0.8$, $\phi_A = 0.05$ where d_A is so low that active particles are basically trapped (see also supplementary video). Other parameters are $M_0^A = M_0^B = 50$. Each point has been obtained as the average of five different simulations started with different initial conditions.

ϕ and ϕ_A. No data is shown for $\phi_A = 0.01$, as the number of active particles is too small for meaningful averages. We observe a clear correlation between d_A and the crystallization in the system: the higher X_f, the smaller is the maximum displacement of active particles until, for the extreme case of $\phi = 0.8$ and $\phi_A = 0.05$ active particles are trapped inside a big cluster and have a very small maximum displacement (see also supplementary video).

B. Active bath: how passive particles can suppress collective migration

Inelastic collisions in systems which are composed solely of active particles can lead to collective motion. This has been shown by particle based models, e.g.[41], microscopic field theoretical models[20] and phase field models[42,43]. In all these models the state of collective motion is characterized by the translational order parameter $\phi_T = 1/N_A \left| \sum_{i=1}^{N_A} \hat{\mathbf{v}}_A^i(t) \right|$ being close to one, with $\hat{\mathbf{v}}_A^i(t)$ the unit velocity vector for the active particle i at time t. We here analyze the stability of the state of collective motion, if passive particles are introduced in the system. How do the relative and absolute densities and the mobility of the passive particles affect this state?

To consider a dense system we fix $\phi = 0.9$. We further set $\phi_A = 0.9$ and vary the mobility of the few passive particles M_0^B. For low mobilities they act as fixed objects and the results can be compared with experimental studies for active colloids in disordered environments[7], which show a suppression of collective motion. Also in our simulations the active system does not reach a state of collective motion, as shown from the time series of ϕ_T (figure 4(b)). However, the situation changes if the passive particles are mobile. Figure 4(a) shows the average velocity $\tilde{\mathbf{v}}_B$ of the passive particles as a function of their mobility. Increasing M_0^B, the average passive particles velocity $\tilde{\mathbf{v}}_B$ also increases, meaning that passive particles are transported from the active ones. For $M_0^B > 30$ a state of collective migration is reached (figure 4(b)), even though the time required to reach it is larger than in the homogeneous case $\phi_A = 1$ (no passive particles present).

We now fix the mobility $M_0^B = 70$ and vary ϕ and ϕ_A. We reduce ϕ down to 0.7, a limit for which a state of collective migration would still be reached in an homogeneous active system ($\phi_A = 1$), as seen from the purple lines in figure 5. For $\phi = 0.9$ a state of collective migration is reached for $\phi_A = 0.9$ but with a longer transient phase than for the homogeneous case (green line in figure 5(c)). For $\phi_A = 0.8$ we already see a small perturbation from the

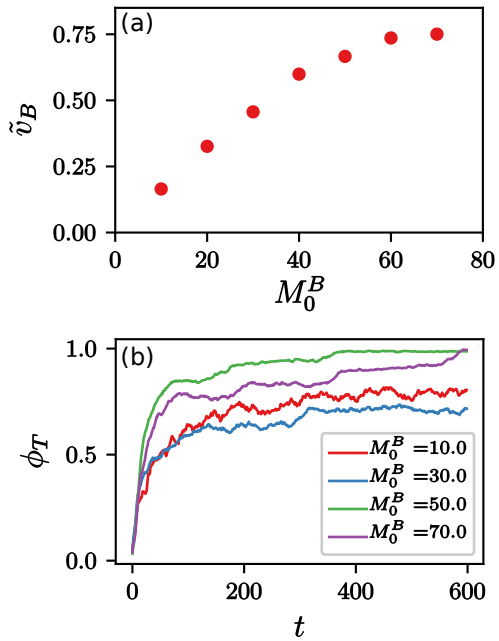

FIG. 4. (a) Average velocity $\tilde{v}_B$ of passive particles as a function of their mobility in an active bath with $\phi = \phi_A = 0.9$. $\tilde{v}_B$ increases almost linearly for small M_0^B until it starts to saturate at around $M_0^B = 70$. (b) Translational order parameter ϕ_T as a function of time for different mobility M_0^B. For small values of M_0^B there is no collective migration, for intermediate values this state is reached quite fast, whereas for high mobility the transient phase to reach collective migration increases. However simulations are not so numerically stable for small and intermediate values of the mobility and this is why we choose $M_0^B = 70$ for the analysis in figure 5. $M_0^A = 100$ for both cases. The data have been obtained as the average of ten different simulations started with different initial conditions.

unit value for ϕ_T and for $\phi_A = 0.7$ collective migration is no longer reached. We here observe the accumulation of passive particles in certain regions, see also figure 6(d). This hinders the active particles from following a straight trajectory and thus the formation of collective migration. Things change by reducing the total density to $\phi = 0.8$. The state of collective migration is not reached, independent of the value of ϕ_A (figure 5(b)). However, for high relative density $\phi_A = 0.9$, green curve in figure 5(b) a new state is formed, where the translational order parameter ϕ_T is at least locally close to one. This new state is discussed below and can be seen in the snapshots in figures 6(a) and (b). For $\phi = 0.7$ (figure 5(a)) a decrease in ϕ_A leads to a decrease of ϕ_T. In this situation there is enough empty space

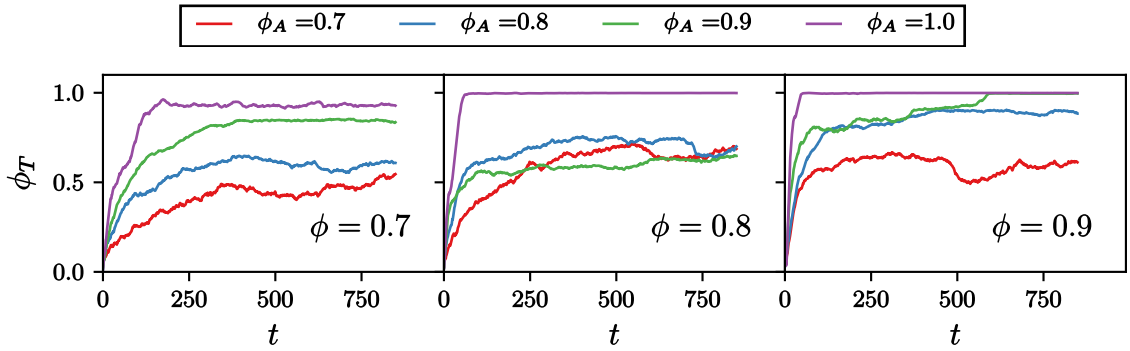

FIG. 5. Translational order parameter ϕ_T as a function of time for different values of ϕ and ϕ_A. The purple curve corresponds to the case $\phi_A = 1$, i.e. no passive particles present. We see that in all other cases the state of collective migration is reached later (longer transient phase) or not reached at all, especially for lower ϕ_A (red curves). Other parameters are $M_0^A = 100$ and $M_0^B = 70$. The data have been obtained as the average of ten different simulations started with different initial conditions.

in the system to allow active particles to change their trajectories when interacting with passive ones. This causes a perturbation that gets bigger as the number of passive particles increase, leading to a decrease of ϕ_T.

A more detailed investigation of the intermediated regime with $\phi = 0.8$ and $\phi_A = 0.9$ is shown in figure 6(a) and (b), showing an intermediate state with two regions of active particles moving in opposite direction. The regions are separated by passive particles. This separation prevents the alignment of the collectively migrating domains. This state can be seen as a local flocking state. It is more stable in figure 6(a), persisting for the whole simulation time, and less stable in figure 6(b), where the alignment of passive particles will be destroyed after a while and a transition to collective migration follows (see supplementary video). However, even if this collective migration state is reached the passive particles are not randomly distributed. As see in figure 6(c) they form chains, which persist over longer periods of time and are transported by the active particles. If the number of passive particles is increased $\phi_A = 0.7$ a clustering of passive particles within the active bath can be observed, see figure 6(d). These new states and patterns are characteristic for binary mixtures and should be explored further, both numerically and experimentally.

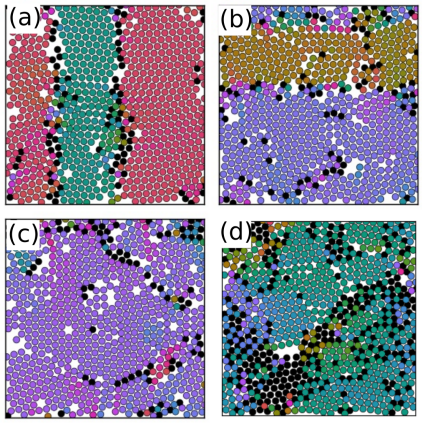

FIG. 6. The color code corresponds to the single particle velocity. (a) Snapshot of a state of local flocking, with two macro regions of active particles having exactly opposite orientation. This state can last for a long time thanks to the presence of passive particles at the boundary between the two regions (see also supplementary video). (b) Another state of local flocking. Here, less passive particles are accumulated at the boundary between the moving active regions. The situation is less stable and transforms in a situation of global collective motion (c), in which passive particles form chains, which persist over longer periods of time. (d) Passive particles forming clusters in an active bath. (a) - (c) regime $\phi = 0.8$, $\phi_A = 0.9$, (d) regime $\phi = 0.9$, $\phi_A = 0.7$.

IV. CONCLUSIONS

In summary, our microscopic field theoretical approach for binary mixtures of interacting active and passive particles has been used to investigate a wide spectrum from dilute systems $\phi < 0.7$ to dense systems $\phi > 0.7$ with a relatively low fraction of active particles $\phi_A < 0.2$ (active doping) and a relatively high fraction $\phi_A > 0.7$ (active bath), respectively. We have demonstrated with one and the same model a variety of known phenomena, such as enhanced crystallization via active doping[3,21] and suppressed crystallization in dense systems[3]. We also analyzed the limits of collective migration, which for the special case of immobile passive particles qualitatively reproduce the results in[7]. Within the experiments in[3] and in our simulations the suppression of collective migration sensitively depends on the fraction of immobile passive particles. Within the experimentally less explored state of mobile passive particles we found new phenomena. For fractions of passive particles, for which collective migration is suppressed if the passive particles are immobile, collective motion is still possible

if the mobility of these particles is large enough. But there are also intermediate regime, characterized by local flocking states, where regions of active particles are separated by boundary layers of passive ones. We further found chains of passive particles and clusters which persist for a relatively long time. A rigorous classification of these states remains open and should be addressed with experimental investigations.

As already pointed out, the proposed microscopic field theoretical model can easily be modified to consider more than two species, species with different size and interaction potential and active species with different self-propulsion velocities, which makes the approach a generic tool to study active systems in complex environments. Also hydrodynamic interactions have already be considered together with a (passive) phase field crystal model[30,44] and they could also be included in our model.

ACKNOWLEDGMENTS

This work is funded by the European Union (ERDF) and the Free State of Saxony via the ESF project 100231947 (Young Investigators Group Computer Simulation for Materials Design - CoSiMa). We used computing resources provided by JSC within project HDR06.

REFERENCES

[1]A. Das, A. Polley, and M. Rao, Phys. Rev. Lett. **114**, 068306 (2016).

[2]J. Stenhammar, R. Wittkowski, D. Marenduzzo, and M. E. Cates, Phys. Rev. Lett. **114**, 1 (2015).

[3]F. Kümmel, P. Shabestari, C. Lozano, G. Volpe, and C. Bechinger, Soft Matter **11**, 1 (2015).

[4]A. Wysocki, R. G. Winkler, and G. Gompper, New J. Phys. **18**, 123030 (2016).

[5]M. Zeitz, K. Wolff, and H. Stark, The European Physical Journal E **40**, 23 (2017).

[6]A. Morin, D. Lopes Cardozo, V. Chikkadi, and D. Bartolo, Phys. Rev. E **96**, 042611 (2017).

[7]A. Morin, N. Desreumaux, J.-B. Caussin, and D. Bartolo, Nat. Phys. **13**, 63 (2017).

[8]M. C. Marchetti, J. F. Joanny, S. Ramaswamy, T. B. Liverpool, J. Prost, M. Rao, and R. A. Simha, Rev. Mod. Phys. **85**, 1143 (2013).

[9]S. Ramaswamy, Annu. Rev. Condens. Matter Phys. **1**, 323 (2010).

[10]C. Bechinger, R. Di Leonardo, H. Löwen, C. Reichhardt, G. Volpe, and G. Volpe, Rev. Mod. Phys. **88**, 045006 (2016).

[11]G. Briand, M. Schindler, and O. Dauchot, arXiv:1709.03844 (2017).

[12]E. Lushi and C. S. Peskin, Comput. Struct. **122**, 239 (2013).

[13]H. Wioland, F. G. Woodhouse, J. Dunkel, J. O. Kessler, and R. E. Goldstein, Phys. Rev. Lett. **110**, 268102 (2013).

[14]C. J. O. Reichhardt and C. Reichhardt, New J. Phys. **20**, 025002 (2017).

[15]C. Reichhardt and C. J. O. Reichhardt, J. Phys.: Condens. Matter **30**, 015404 (2018).

[16]A. Kaiser, H. H. Wensink, and H. Löwen, Phys. Rev. Lett. **108**, 268307 (2012).

[17]A. Kaiser, K. Popowa, H. H. Wensink, and H. Löwen, Phys. Rev. E **88**, 022311 (2013).

[18]S. R. McCandlish, A. Baskaran, and M. F. Hagan, Soft Matter **8**, 2527 (2012).

[19]A. M. Menzel and H. Löwen, Phys. Rev. Lett. **110**, 55702 (2013).

[20]F. Alaimo, S. Praetorius, and A. Voigt, New J. Phys. **18**, 083008 (2016).

[21]R. Ni, M. A. Cohen Stuart, M. Dijkstra, and P. G. Bolhuis, Soft Matter **10**, 6609 (2014).

[22]B. van der Meer, M. Dijkstra, and L. Filion, Soft Matter **12**, 5630 (2016).

[23]X. L. Wu and A. Libchaber, Phys. Rev. Lett. **84**, 3017 (2000).

[24]C. Valeriani, M. Li, J. Novosel, J. Arlt, and D. Marenduzzo, Soft Matter **7**, 5228 (2011).

[25]D. F. Hinz, A. Panchenko, T.-Y. Kim, and E. Fried, Soft Matter **10**, 9082 (2014).

[26]J. Swift and P. C. Hohenberg, Phys. Rev. A **15**, 319 (1977).

[27]P. Chan, N. Goldenfeld, and J. Dantzig, Phys. Rev. E **79**, 035701 (2009).

[28]J. Berry and M. Grant, Phys. Rev. Lett. **106**, 175702 (2011).

[29]M. J. Robbins, a. J. Archer, U. Thiele, and E. Knobloch, Phys. Rev. E **85**, 061408 (2012).

[30]S. Praetorius and A. Voigt, J. Chem. Phys. **142**, 154904 (2015).

[31]A. M. Menzel, T. Ohta, and H. Löwen, Phys. Rev. E **89**, 022301 (2014).

[32]K. R. Elder, M. Katakowski, M. Haataja, and M. Grant, Phys. Rev. Lett. **88**, 245701 (2002).

[33]K. R. Elder and M. Grant, Phys. Rev. E **70**, 051605 (2004).

[34]K. R. Elder, N. Provatas, J. Berry, P. Stefanovic, and M. Grant, Phys. Rev. B **75**, 64107 (2007).

[35]S. van Teeffelen, R. Backofen, A. Voigt, and H. Löwen, Phys. Rev. E **79**, 051404 (2009).

[36]R. Backofen, A. Rätz, and A. Voigt, Phil. Mag. Lett. **87**, 813 (2007).

[37]S. Praetorius and A. Voigt, SIAM Journal on Scientific Computing **37**, B425 (2015).

[38]S. Vey and A. Voigt, Comput. Visualization Sci. **10**, 57 (2007).

[39]T. Witkowski, S. Ling, S. Praetorius, and A. Voigt, Advances in Computational Mathematics **41**, 1145 (2015).

[40]M. Skoge, A. Donev, F. H. Stillinger, and S. Torquato, Phys. Rev. E **74**, 041127 (2006).

[41]D. Grossman, I. S. Aranson, and E. Ben Jacob, New J. Phys. **10**, 023036 (2008).

[42]J. Löber, F. Ziebert, and I. S. Aranson, Scientific Reports **5**, 9172 (2015).

[43]W. Marth and A. Voigt, Interface Focus **6**, 20160037 (2016).

[44]V. Heinonen, C. V. Achim, J. M. Kosterlitz, S.-C. Ying, J. Lowengrub, and T. Ala-Nissila, Phys. Rev. Lett. **116**, 024303 (2016).